The 20-pS chloride channel of the human airway epithelium

Marek Duszyk,* Andrew S. French,* and S. F. Paul Man‡
Departments of *Physiology and ‡Medicine, University of Alberta, Edmonton, Alberta T6G 2H7 Canada

ABSTRACT The single-channel inside-out patch clamp technique was used to characterize chloride channels in the apical membranes of human airway epithelial cells maintained in primary culture. Patches were obtained from single isolated cells or from cells at the edges of confluent groups. The channel seen most often, in 24% of all patches, had a conductance of ~20 pS and had a linear current-voltage relationship in symmetric chloride solutions. The anion selectivity sequence for the channel was $NO_3^- > Cl^- > HCO_3^-$, and it was impermeable to gluconate ions, indicating that the channel diameter lies between 4.7 and 5.5 Å. Current through the channel saturated at high chloride concentrations, and the relationship between channel current and chloride concentration could be approximated by the Michaelis-Menten equation. Analysis of the channel's anion permeability and its current vs. concentration relationship indicates that it can be described by the one-ion channel theory, with a relatively weak binding site inside the channel. Histograms of channel open and closed durations were constructed using the log binning technique and could be well fitted by triple exponential distributions, suggesting that the channel has at least three open and three closed states.

INTRODUCTION

Epithelial airway cells generate several ion fluxes which are important for mucociliary clearance and other physiological functions. Although there are regional and species differences, a general description of these ionic movements is now possible (Welsh, 1987). The major driving force for ion movements is a sodium-potassium ATPase in the basolateral membrane, which produces low intracellular sodium concentration and a high intracellular potassium concentration. The internal chloride ion concentration is elevated by a passive Na^+-K^+-$2Cl^-$ cotransport system in the basolateral membrane, driven by the high interstitial sodium, and this high intracellular chloride concentration, together with the electrical gradient, favors passive chloride exit through the apical membrane via chloride ion channels.

Chloride channels of 20 and 40 pS conductance have been identified previously in airway epithelia by Frizzell et al. (1986, 1987), whereas Shoemaker et al. (1986) have described four different kinds of chloride channels in airway epithelia with conductances of 10, 20, 40, and 250 pS at physiological chloride concentrations. The 40-pS chloride channel rectifies in symmetric chloride solutions, and its gating properties have been characterized in more detail (Welsh, 1986*a* and *b*; Schoumacher et al., 1987; Li et al., 1988).

In a survey of normal human airway epithelial cells we have found the 20-pS chloride channel to be the most common ion channel of the apical membrane, occurring in 24% of successful patches (n = 495 patches). This paper describes some of the permeation properties and kinetic behavior of the channel.

MATERIALS AND METHODS

Cells

Epithelial tissues were obtained from the partially resected nasal turbinates of 26 normal human subjects. The tissues were treated with 0.1% protease and 0.1% DNase in calcium-free minimum essential medium (MEM) at 4°C for 16–24 h. The enzymes were neutralized by adding 10% fetal bovine serum (FBS) to the mixture for 30 min, and then the cells were detached from the epithelial strips by gentle mechanical agitation. Free cells were filtered through a Nitex nylon mesh (60 μm), centrifuged at 150 *g* for 10 min, pelleted, and then resuspended in 10% FBS in MEM. Trypan blue exclusion was used to test viability, which was normally >90%. The cells were washed once more and then plated at low density on Falcon Primaria plates at 37°C in a culture medium containing MEM-F12 supplemented with insulin (1 mg/ml), transferrin (7.5 mg/ml), hydrocortisone (1 mM), cholera toxin (10 ng/ml), T_3 (0.1 nM), epidermal growth factor (2.5 mg/ml), endothelial cell growth substance (10 μm/ml), and antibiotics (gentamycin 50 μg/ml, streptomycin 50 μg/ml, and penicillin-G 50 μg/ml) (Wu et al., 1985). Experiments were performed on isolated cells, or those at the edges of confluent sheets. The temperature was kept at 37 ± 1°C during all experiments by means of a thermostatically controlled stage. Experiments were performed with cells not more than 6 d old, usually between 1 and 4 d after plating.

Channel recording

Single channel currents were recorded from excised patches of apical membrane in the inside-out configuration using a model EPC-7 ampli-

0006-3495/90/02/223/08 $2.00

fier (Adams & List Associates, Ltd., Great Neck, NY) (Hamill et al., 1981). Pipettes were fabricated from thick-walled microfilament borosilicate glass using a two-stage pipette puller (Narishige Scientific Laboratory, Tokyo, Japan), coated with Sylgard (Dow Corning Corp., Midland, MI) and fire polished with a microforge (Narishige Scientific Laboratory). Pipette resistances were 16–20 MΩ when filled with 140 mM NaCl solution and gave seal resistances of ~30 GΩ. To minimize junction potentials, a NaCl-agar-filled bridge was used to connect the reference electrode to the bathing solution. For experiments with different Cl^- concentrations the junction potential at the reference electrode was calculated from the Henderson equation (MacInnes, 1939) and subtracted from the measured membrane potential to obtain the potential across the patch. Pipette offset potentials were measured and corrected before forming a seal. All potentials are reported relative to zero in the extracellular solution, and positive currents are outwards throughout.

Channel current signals from the amplifier were filtered using a 10-kHz bandwidth Bessel filter and fed into a digital VCR recorder adaptor (PCM-1, Medical Systems Corp., Great Neck, NY) and stored on video tape. A digital computer sampled the data at 10 kHz with a 12-bit analog-to-digital convertor. During data processing, the recordings were usually further filtered using either a 5- or 1-kHz Gaussian digital filter.

Solutions

The solutions used in the experiments contained 140 mM NaCl, 2 mM $CaCl_2$, 1 mM $MgCl_2$, 5 mM Hepes, and the pH was adjusted to 7.2 with NaOH or KOH. In experiments with ion permeation, chloride ions were replaced by NO_3^-, HCO_3^-, or gluconate ions. In other experiments sodium ions were replaced by choline, Cs^+, or K^+. To investigate the influence of chloride concentration on channel current, the chloride concentration in the bath solution was changed from 50 to 600 mM. The osmolarity of the low-chloride bath solution was adjusted by the addition of sucrose. The low-calcium solution contained 140 mM NaCl, 1 mM $CaCl_2$, 2 mM $MgCl_2$, 10 mM Hepes, and 10 mM EGTA, and the pH was adjusted to 7.2 with NaOH. Estimation of the free calcium concentration in the low-calcium solution, taking into account ionic strength, pH, temperature, and magnesium concentration, gave a value of ~11 nM (Stockbridge, 1987).

Changes in the bath solution were accomplished by moving the pipette tip into a small chamber, separated from the main dish. A flow system with very small dead space allowed rapid exchange of solutions in this small volume.

Determination of reversal potentials

Reversal potentials were determined from current-voltage relationships plotted for different ions. Relative ion permeabilities were calculated from Eq. 1 assuming that two anions were present (Hille, 1984):

$$V_o = -\frac{RT}{F}\ln\frac{[Cl^-]_o + P_A/P_{Cl}[A^-]_o}{[Cl^-]_i + P_A/P_{Cl}[A^-]_i}, \quad (1)$$

where subscripts o and i denote outside and inside solutions, respectively, P_A is the permeability of an anion, and R, T, and F are the gas constant, temperature, and Faraday constant, respectively.

Data analysis

The procedures used for computer data analysis were based largely on those described by Colquhoun and Sigworth (1983). The half-amplitude criterion was used as a threshold to distinguish between open and closed states. Event durations were corrected for filter rise-time by a polynomial approximation (Colquhoun and Sigworth, 1983; Eq. 17). Distributions of open and closed times were created and the probability of the channel being in the open state was calculated. Only openings longer than the filter dead-time were used to compute the mean channel current amplitude. Histograms of open and closed intervals were created using the square root of the number of events vs. the log binwidth of event durations (Sigworth and Sine, 1987). Distributions were corrected for sampling promotion error using the probabilistic redistribution method of Korn and Horn (1988). The distributions were fitted with probability density functions of the form:

$$f(t) = \sum_{j=1}^{k} a_j/\tau_j \exp(-t/\tau_j), \quad (2)$$

where k is the number of exponential components, and a_j and τ_j are the fitted amplitude and time constant parameters. The number of fitted parameters for a given value of k is $2k - 1$. The data were fitted using the maximum likelihood method (Colquhoun and Sigworth, 1983), assuming that each event had a duration equal to the midpoint of its bin. The number of significant components k was determined using the Akaike likelihood ratio test (Korn and Horn, 1988).

THEORY

Ion movement through channels

The movement of ions through channels in cell membranes may be described by models based on discrete or continuum theories. The discrete theory models a channel as a set of occupancy states separated by energy barriers (see e.g. Läuger, 1987). Transitions between the states are characterized by first-order reaction equations. Solutions of this problem depend on the number of energy wells and barriers. The current is expressed as a function of rate constants for transitions between the states and the ionic concentrations on both sides of the channel. This theory has recently been reviewed by Cooper et al. (1988*a* and *b*).

Continuum theory is based on the Nernst-Planck electrodiffusion equation, which can be written in the following form (Levitt, 1986):

$$J = -DS(dC/dX + C\,d\nu/dX),$$

where

$$\nu = zF/(RT)(\Psi + \Phi) = \psi + \phi. \quad (3)$$

J is the ionic flux through the channel, z is the ion valency, $S(x)$ is the area available for the ion as a function of position within the channel, $D(x)$ is the ionic diffusion coefficient, $C(x)$ is the ion concentration, $\Psi(x)$ is the applied external voltage, $\Phi(x)$ is the intrinsic electrochemical potential, ν, ψ, and ϕ are the dimensionless: total, external, and intrinsic potentials, respectively. The channel current is given by $I = ezJ$, where e is the electronic charge.

In the steady state, Eq. 3 can be integrated to yield:

$$J = [C_1 \exp(\psi_1) - C_2]/H, \quad (4)$$

where

$$H = \int_{-\infty}^{+\infty} \exp(\nu)/(DS)\,dX. \quad (4a)$$

The integration ranges from the bulk solution on side 1 to the bulk solution on side 2 (Fig. 1) so that $C(-\infty) = C_1$, $C(\infty) = C_2$, $\nu(-\infty) = \psi_1$,

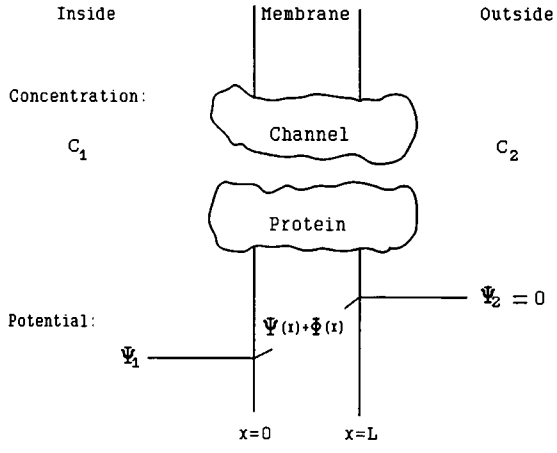

FIGURE 1 Schematic diagram of a hypothetical membrane channel (further explanation in text).

$\nu(\infty) = \psi_2 = 0$. Eq. 4 gives a general description of ionic movement through a channel, whereas the channel itself is characterized by the integral H.

The constant field theory (Hille, 1984) assumes independent ion movement and cannot explain phenomena such as the saturation of ion fluxes with increasing concentration. This deviation can be explained by assuming that ions must bind to certain sites within the channel and that sites can only bind one ion at a time. In particular, the one-ion channel is defined as a channel which can contain only one ion at a time, but which can have many bindings sites (Hille, 1984). The solution of the Nernst-Planck equation for this class of channels is given by Levitt (1986):

$$J = [C_1 \exp(\psi_1) - C_2]/[H(1)(1 + LC_1M)], \quad (5)$$

where L is the channel length,

$$B(x) = \exp[\phi(x)]/S(x) \quad (5a)$$

$$H(y) = L\int_0^y D^{-1} B(x) \exp[\psi(x)]\,dx, \quad (5b)$$

$$M(\psi, C_1/C_2) = \int_0^1 B^{-1} \exp[-\psi(x)]\{\exp(\psi_1) - C_2H(x)[\exp(\psi_1) - 1]/[C_1H(1)]\}\,dx. \quad (5c)$$

If C_2 is constant, Eq. 5 can be transformed into the following form:

$$I = I_m(C_1 - A)/(C_1 + K) \quad (6)$$

where A, I_m, and K are functions of the applied voltage and channel parameters.

Eq. 6 has three parameters: I_m, A, and K. A is determined by the ion concentration and membrane potential, whereas I_m and K are related in a unique manner to the size and energy profile of the channel and can be determined by fitting Eq. 6 to the experimental relationship between channel current and ionic activity.

In a generalized constant field theory (Levitt, 1986) the function $B(x)$ (Eq. 5a) is assumed to be a constant (B_o) except for a narrow region where $B(x)$ is small. This region would correspond to a potential energy well ($|\phi| \gg 1, \phi < 0$) inside the channel. The applied voltage $\psi(x)$ is assumed to vary linearly inside the channel according to the equation

$$\psi = \psi_1(1 - x/L), \quad (7)$$

where $\psi_1 = xEF/(RT)$.

If we assume that the diffusion coefficient $D(x)$ is a constant, then A can be calculated as $A = C_2 \exp(-\psi_1)$, and the parameters I_m and K are related to the channel size and energy profile by:

$$I_m = ezD \exp(\psi_1)/[E_pL^2(E_p + B_o/B_w)],$$
$$K = [B_o - LC_2(E_p - 1)]/[L(E_p + B_o/B_w)], \quad (8)$$

where

$$E_p = (\exp(\psi_1) - 1)/\psi_1, \qquad B_w = \int_{well} B^{-1}\,dx.$$

RESULTS

From a total of 495 successful patches, four types of chloride channels were identified. The 20-pS channel (15–35 pS range) was found most often (117 channels) but we also observed 40-pS rectifying chloride channels (four channels), large chloride channels with conductances of ~300 pS (eight channels), and small chloride channels with conductances of ~10 pS (21 channels). For all of these conductance measurements, the pipette and the bath contained 140 mM NaCl, 2 mM $CaCl_2$, 1 mM $MgCl_2$, and 5 mM Hepes (pH 7.2). The selectivity of the channels was tested by replacing sodium with choline in the bathing solution. Choline, which blocks sodium channels in human airway epithelia (Duszyk et al., 1989) had no effect on the currents measured through the present channels, indicating that they conduct chloride ions. Fig. 2 shows typical recordings of the 20-pS chloride channel in different solutions.

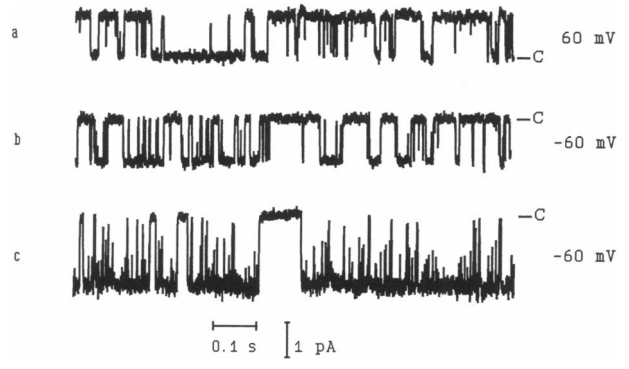

FIGURE 2 Examples of single channel recordings of the 20-pS chloride channel in human airway epithelia. (*a*) Membrane potential +60 mV in symmetric solutions containing 146 mM chloride. (*b*) −60 mV and symmetric 146 mM chloride. (*c*) −60 mV, 146 mM chloride in the pipette and 600 mM chloride in the bath. The closed condition is indicated by the letter *C* in each case.

The distribution of channel conductances in the range 15–35 pS in symmetric 146 mM chloride is shown in Fig. 3. The distribution showed evidence of a bimodal structure and was fitted with a sum of two Gaussian functions of 20.5 ± 3.1 pS and 31.9 ± 2.6 pS (mean ± S.D.). However, all of the channels shown in Fig. 3 were voltage independent and had similar probabilities of opening. All of the results presented in the following sections were obtained from channels with conductances between 17.5 and 23.5 pS.

Anion selectivity

Fig. 4 shows current-voltage relationships for the 20-pS chloride channel in symmetric chloride solution, and when the NaCl in the bath was replaced by equal amounts of $NaNO_3$, $NaHCO_3$, or sodium gluconate. In symmetric NaCl solutions, the channel had a linear current-voltage relationship with zero reversal potential. The reversal potential with NO_3^- in the bath was 15.3 mV, indicating that NO_3^- is more permeant than Cl^-. On the other hand, HCO_3^- had a reversal potential of −16.1 mV, indicating that this anion is less permeant than Cl^-. Negative ion currents were not observed with gluconate ions in the bath, indicating that gluconate ions are not measurably permeable through the channel. The permeability ratios P_A/P_{Cl} calculated from Eq. 1 for NO_3^- and HCO_3^- were equal to 1.79 and 0.52, respectively.

In summary, the anion selectivity order for the 20-pS channel was $NO_3^- > CL^- > HCO_3^-$ while it was not permeable to gluconate. The diffusion coefficients of Cl^- and NO_3^- in water solution are 2.03×10^{-9} m^2/s and 1.90×10^{-9} m^2/s, respectively (Robinson and Stokes, 1965). Therefore, the fact that the NO_3^- anion is more permeable than Cl^- through the channel suggests that diffusion is not the main determinant of channel permeability, and that anions must interact with the channel itself rather than simply diffuse through a water-filled tube.

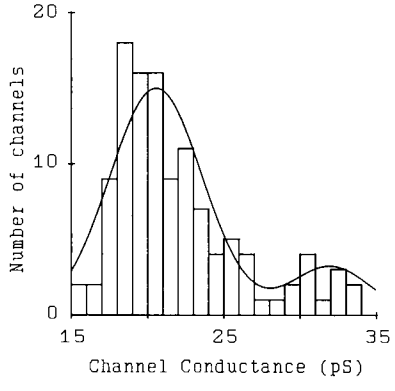

FIGURE 3 Distribution of chloride channel conductances in the range 15–35 pS. The distribution is fitted with a sum of two Gaussian functions having mean conductances of 20.5 and 31.9 pS.

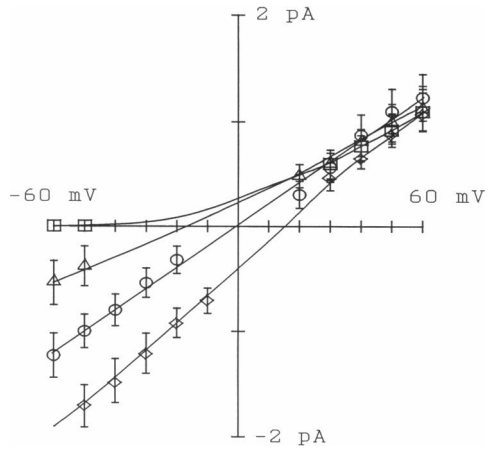

FIGURE 4 Current-voltage relationships for a 20-pS anion channel. The pipette contained 140 mM NaCl and the bath contained 140 mM sodium gluconate (*squares*), 140 mM $NaHCO_3$ (*triangles*), 140 mM NaCl (*circles*), and 140 mM $NaNO_3$ (*diamonds*). The remaining components in the pipette and the bath were 2 mM $CaCl_2$, 1 mM $MgCl_2$, and 5 mM Hepes (pH 7.2). The data points show means and standard deviations from at least three different experiments in each case. Solid lines through the data points were drawn by eye except for the symmetric case, where linear regression was used. Negative currents were not observed with gluconate in the bath solution.

To test the effects of cations on channel permeability, we replaced the sodium ions in the bath with K^+, Cs^+, or choline ions. These replacements gave no measurable effects on the channel current (data from five patches), indicating that cations are not involved in channel permeation.

Dependence of channel current on ionic concentration

Current-voltage relationships for different chloride concentrations are shown in Fig. 5. The pipette contained 140 mM NaCl, 2 mM $CaCl_2$, 1 mM $MgCl_2$, and 5 mM Hepes (pH 7.2), whereas the total concentration of chloride in the bath was varied from 50 to 600 mM by varying the amount of NaCl, and adjusting the osmolarity with sucrose. The figure presents mean values from three different experiments for each data point. Fig. 6 shows a plot of channel current at a potential of −50 mV, as a function of chloride activity. The channel current saturated at high chloride activities, and the data were well fitted by Eq. 6, with the best fit being obtained for

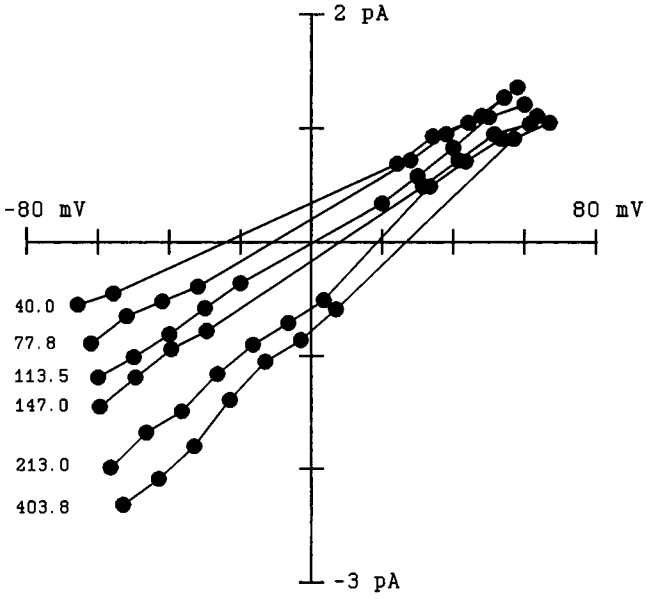

FIGURE 5 Current-voltage relationships at different chloride concentrations. The pipette contained 140 mM NaCl, 2 mM $CaCl_2$, 1 mM $MgCl_2$, and 5 mM Hepes (pH 7.2). The data show mean values from three different experiments. Standard deviations ranged from 0.09 to 0.28 pA but are omitted for clarity. Membrane potentials have been corrected for the junction potential at the reference electrode (see Materials and Methods). Values of the total chloride activity (millimolar) in the bath are indicated next to each data set. The cations in the bath were 2 mM Ca^{2+}, 1 mM Mg^{2+}, and the balance was Na^+. The bath also contained 5 mM Hepes (pH 7.2).

parameters of J_m = 3.90 pA, and K = 247.7 mM (solid line). The fact that the data could be well approximated by Eq. 6 indicates that this channel can be described by the one-ion channel hypothesis.

Channel gating

The probability of the channel being open as a function of transmembrane potential is shown in Fig. 7. The data present mean values and standard deviations from 16 recordings. Over the range of tested voltages (±60 mV), the probability of being open was almost constant at ~0.27, indicating that channel activity is independent of voltage. To test the effect of calcium on channel activity, the bath solution was changed from one containing 2 mM Ca^{++}, to another solution containing 20 nM Ca^{++}. In six different experiments, there was no measurable effect on channel open probability.

Kinetic analysis of channel activity was performed on data obtained from patches where there was clearly only one channel present and where the noise level allowed a 5-kHz filter to be used (23 different recordings). The

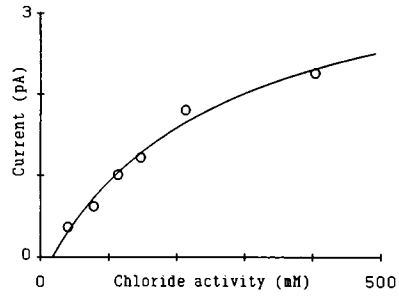

FIGURE 6 The relationship between channel current at −50 mV and chloride activity. The pipette contained 113.5 mM Cl^- activity while the bath solution varied from 40 to 403.8 mM Cl^- activity. These data points were obtained from Fig. 5 by linear interpolation between adjacent values. The solid line represents the best fit of Eq. 6 to the data and corresponds to the parameters I_m = 3.90 pA and K = 247.7 mM.

number of transitions between open and closed states for each recording varied between 857 and 23,612 events. An example of kinetic analysis is shown in Fig. 8. Distributions of open and closed states were fitted by Eq. 2. In 44% of recordings the best fit to the open durations was obtained from the sum of two exponentials, whereas 56% of the data were best fitted with the sum of three exponentials. The time constants (mean ± S.D.) for the sum of three exponentials were: 0.17 ± 0.08, 2.49 ± 2.10, and 8.55 ± 8.56 ms.

For the closed durations, 83% of recordings were best fitted by a sum of three exponentials with time constants of 0.16 ± 0.07, 1.53 ± 1.61, and 17.22 ± 14.42 ms, whereas a sum of two exponentials fitted the remaining 17% of the recordings. No relationship could be found

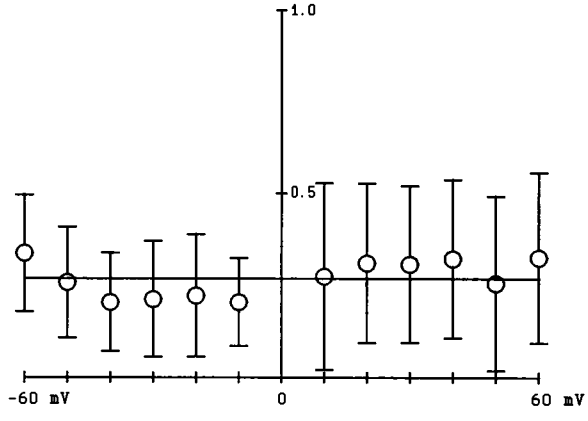

FIGURE 7 The probability of the 20-pS chloride channel being open as a function of membrane potential. The data points show means and standard deviations from 16 recordings. The solid line shows the mean value for all of the data (p = 0.27).

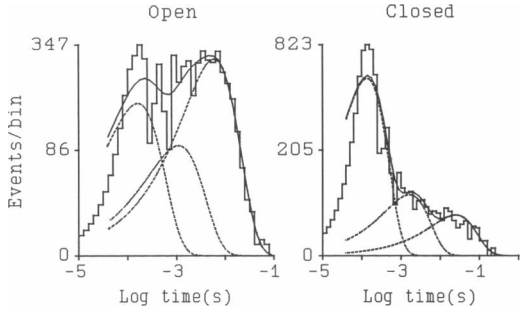

FIGURE 8 Distributions of open and closed durations of a 20-pS chloride channel, plotted on square root vs. log time axes with 10 bins per decade. The data were obtained from a channel held at −60 mV. The total number of events was 6,364. Solid lines represent fits from Eq. 2 with sums of three exponentials in both cases. The dashed lines show the separate components of the fits, with their peaks corresponding to individual time constants along the abscissa.

between kinetic parameters and membrane potential, reflecting the lack of dependence of open probability on membrane potential.

DISCUSSION

The 20-pS chloride channel was seen in 24% of all successful patches on the apical membranes of airway epithelial cells, and was the most common channel seen in this membrane. This channel is probably identical to the 20-pS chloride channel reported previously in epithelial cells (Frizzell et al., 1986, 1987).

The conductance of airway epithelia lies in the range 2–10 mS/cm^2, with at least 60% of the current being carried by chloride ions. However, rates of ionic movement in cultured cells can be less than this by a factor of 10 (Welsh, 1987). The range of chloride conductances anticipated for apical membranes of cultured cells is therefore 0.12–0.6 mS/cm^2. Chloride conductance in the apical membranes of nasal epithelial cells has recently been estimated to be 0.7 mS/cm^2 (Willumsen and Boucher, 1989). The area of the membrane patches used in the present experiments was estimated from the tip resistance, assuming that the patch diameter lies between the pipette diameter and that of an Ω-shaped patch (Sakmann and Neher, 1983), to be 1–5 μm^2. Because we found 20-pS channels in 24% of patches, the predicted apical membrane conductance due to 20-pS channels is 0.096–0.48 mS/cm^2, suggesting that 20-pS channels could account for a large proportion of total chloride conductance in the apical membrane. Whole cell chloride currents have recently been measured in canine tracheal epithelial cells (Schoppa et al., 1989). These recordings showed little evidence of rectification, suggesting that a majority of chloride ions flow through nonrectifying channels.

Anion selectivity

The selectivity of an ion channel is determined by interactions between the ion and the channel protein, and by the change in free energy associated with the movement of ions from the bath to the channel (dehydration energy). Dehydration energies for anions were reported by Wright and Diamond (1977) to be 79 and 69 Kcal/mol for Cl^- and NO_3^-, respectively (or 128.3 and 112.1 kT per molecule). Data for HCO_3^- and gluconate ions are unavailable. The smaller dehydration energy for the NO_3^- ion, which is more permeant than chloride, suggests that the energy necessary to dehydrate the anion is a major determinant of permeation, and that interactions between the ion and the binding site are smaller than the dehydration energy.

The size of the 20-pS channel can be deduced from the radii of the ions used. The size of the HCO_3^- and gluconate ions can be estimated from three-dimensional space filling models (Stuart, 1934) which, taking into account atomic sizes and bond lengths, give ~4.7 and 5.5 Å. Because HCO_3^- ions are permeant through the channel whereas gluconate ions are not, the diameter of the channel may be estimated to lie between 4.7 and 5.5 Å.

Ion binding in the channel

Fig. 6 shows the channel current as a function of chloride activity. The solid line presents the best fit to Eq. 6. The fitted parameters I_m and K contain four unknown parameters B_o, B_w, D, and L, but values of some of these can be estimated from other measurements. The parameter B_o is equal to $\exp(\phi(x))/S(x)$, where $S(x)$ is the area of the channel. Because the permeability experiments indicate that the channel diameter is 4.7–5.5 Å, we can assume that the channel radius is 2.5 Å, and that $\phi(x) = 0$ at the end of the channel. The value of B_o is then 5.03×10^{18} m^{-2}. The value of the diffusion coefficient in channels has been estimated experimentally (Dani and Levitt, 1981), and theoretically (Jakobsson and Chiu, 1987; Skerra and Brickmann, 1987; Chiu and Jakobsson, 1989). If we assume that D is 5.0×10^{-10} m^2/s, then the corresponding values of B_o/B_w and L are 20.24 and 1.4 nm, respectively. From the ratio B_o/B_w it is possible to calculate the height of the potential energy well in the channel, because the ratio B_o/B_w can be written in the following form:

$$B_o/B_w = \exp[\Delta E/(kT)], \quad (9)$$

where ΔE is the energy barrier inside the channel, and is therefore equal to 3.01 kT.

This value of the energy barrier suggests that interactions between the ion and the binding site inside the channel are not strong. This conclusion agrees with the results of the permeability experiments which indicate that the ion-channel interaction energy is substantially less than the dehydration energy of the ion.

Control of channel gating

Kinetic analysis was performed by the log binning method of Sigworth and Sine (1987), using the Akaike criterion for determination of the minimal number of exponential components k (Korn and Horn, 1988). The distribution of both open times and closed times were usually best approximated by a sum of three components. This suggests that the channel protein has a minimum of three open and three closed states (Colquhoun and Sigworth, 1983).

The kinetic parameters of the channel and the probability of it being open were both independent of membrane potential. In the excised patch situation, the open probability was also apparently independent of intracellular calcium concentration. The factors which control gating of the channel therefore remain unknown. Because the channel seems to make a major contribution to the total chloride permeability of the apical membrane, which in turn is crucially important for normal airway function, the discovery of these gating mechanisms is potentially very important.

We are grateful to Dr. Frederick Sachs for his advice in preparing the manuscript.

Support for this work was provided by the Medical Research Council of Canada and the Alberta Heritage Foundation for Medical Research. The assistance of the Department of Otolaryngology of the University of Alberta Hospital in providing human tissues is gratefully acknowledged.

Received for publication 20 April 1989 and in final form 22 September 1989.

REFERENCES

Chiu, S.-W., and E. Jakobsson. 1989. Stochastic theory of singly occupied ion channels. II. Effects of access resistance and potential gradients extending into the bath. *Biophys. J.* 55:147–157.

Colquhoun, D., and F. J. Sigworth. 1983. Fitting and statistical analysis of single-channel records. *In* Single-Channel Recording. B. Sakmann and E. Neher, editors. Plenum Publishing Corp., New York. 191–263.

Cooper, K. E., P. Y. Gates, and R. S. Eisenberg. 1988*a*. Surmounting barriers in ionic channels. *Q. Rev. Biophys.* 21:331–364.

Cooper, K. E., P. Y. Gates, and R. S. Eisenberg. 1988*b*. Diffusion theory and discrete rate constants in ion permeation. *J. Membr. Biol.* 106:95–105.

Dani, J. A., and D. G. Levitt. 1981. Water transport and ion-water interaction in the gramicidin channel. *Biophys. J.* 35:501–508.

Duszyk, M., A. S. French, and S. F. P. Man. 1989. Sodium channels in the apical membrane of nasal epithelial cells. *Can. J. Physiol. Pharmacol.* 67:Aix.

Frizzell, R. A., D. R. Halm, G. Rechkemmer, and R. L. Shoemaker. 1986. Chloride channel regulation in secretory epithelia. *Fed. Proc.* 45:2727–2731.

Frizzell, R. A., R. A. Schoumacher, and D. R. Halm. 1987. Chloride channel regulation in cystic fibrosis epithelia. *In* Genetics and Epithelial Cell Dysfunction in Cystic Fibrosis. J. R. Riordan and M. Buchwald, editors. Alan R. Liss Inc., New York. 101–113.

Hamill, O. P., A. Marty, E. Neher, B. Sakmann, and F. J. Sigworth. 1981. Improved patch-clamp techniques for high resolution current recording from cells and cell-free membrane patches. *Pfluegers Arch. Eur. J. Physiol.* 391:85–100.

Hille, B. 1984. Ionic channels of excitable membranes. Sinauer Associates, Sunderland, MA.

Jakobsson, E., and S.-W. Chiu. 1987. Stochastic theory of ion movement in channels with single-ion occupancy. Application to sodium permeation of gramicidin channels. *Biophys. J.* 52:33–46.

Korn, S. J., and R. Horn. 1988. Statistical discrimination of fractal and Markov models of single-channel gating. *Biophys. J.* 54:871–877.

Läuger, P. 1987. Dynamics of ion transport systems in membranes. *Physiol. Rev.* 67:1296–1331.

Levitt, D. G. 1986. Interpretation of biological ion channel flux data: reaction rate versus continuum theory. *Annu. Rev. Biophys. Biophys. Chem.* 15:29–57.

Li, M., J. D. McCann, C. M. Lietke, A. C. Nairn, P. Greengard, and M. J. Welsh. 1988. Cyclic AMP-dependent protein kinase opens chloride channels in normal but not cystic fibrosis airway epithelium. *Nature (Lond.).* 331:358–360.

MacInnes, D. A. 1939. The principles of electrochemistry. Reinhold Publishing Corp., Washington, DC.

Robinson, K. R., and R. H. Stokes. 1965. Electrolyte Solutions. Butterworth & Co. Ltd., London.

Sakmann, B., and E. Neher. 1983. Geometric parameters of pipettes and membrane patches. *In* Single-Channel Recording. B. Sakmann and E. Neher, editors. Plenum Publishing Corp., New York. 37–51.

Schoppa, N., S. R. Shorofsky, F. Jow, and D. J. Nelson. 1989. Voltage-gated chloride currents in cultured canine tracheal epithelial cells. *J. Membr. Biol.* 108:73–90.

Schoumacher, R. A., R. L. Shoemaker, D. R. Halm, E. A. Tallant, R. W. Wallace, and R. A. Frizzell. 1987. Phosphorylation fails to activate chloride channels from cystic fibrosis airway cells. *Nature (Lond.).* 330:752–754.

Shoemaker, R. L., R. A. Frizzell, T. M. Dwyer, and J. M. Farley. 1986. Single chloride channel currents from canine tracheal cells. *Biochim. Biophys. Acta.* 858:235–242.

Sigworth, F. J., and S. Sine. 1987. Data transformation for improved display and fitting of single-channel dwell time histograms. *Biophys. J.*52:1047–1054.

Skerra, A., and J. Brickmann. 1987. Simulation of voltage-driven hydrated cation transport through narrow transmembrane channels. *Biophys. J.* 51:977–984.

Stockbridge, N. 1987. EGTA. *Comput. Biol. Med.* 17:299–304.

Stuart, H. A. 1934. Über neue Moleculmodelle. *Z. Phys. Chem.* B27:350–358.

Welsh, M. J. 1986*a*. An apical-membrane chloride channel in human tracheal epithelium. *Science (Wash. DC)*. 232:1648–1650.

Welsh, M. J. 1986*b*. Single apical membrane anion channels in primary cultures of canine tracheal epithelium. *Pfluegers Arch. Eur. J. Physiol.* 407:S116–S122.

Welsh, M. J. 1987. Electrolyte transport by airway epithelia. *Physiol. Rev.* 67:1143–1184.

Willumsen, N. J., and R. C. Boucher. 1989. Shunt resistance and ion permeabilities in normal and cystic fibrosis airway epithelia. *Am. J. Physiol.* 256:C1054–C1063.

Wright, E. M., and J. M. Diamond. 1977. Anion selectivity in biological systems. *Physiol. Rev.* 57:109–156.

Wu, R., J. Yankaskas, E. Cheng, M. R. Knowles, and R. C. Boucher. 1985. Growth and differentiation of human nasal epithelial cells in culture: serum free, hormone-supplemented medium and proteoglycan synthesis. *Am. Rev. Respir. Dis.* 132:311–320.